

Observations of the Binary Microlens Event MACHO-98-SMC-1 by the Microlensing Planet Search Collaboration

S.H. Rhie¹, A.C. Becker^{2,3}, D.P. Bennett^{1,3}, P.C. Fragile¹, B.R. Johnson⁵ L.J. King^{1,3},
B.A. Peterson⁴, J.Quinn¹

(The Microlensing Planet Search Collaboration)

ABSTRACT

We present the observations of the binary lensing event MACHO-98-SMC-1 conducted at the Mt. Stromlo 74" telescope by the Microlensing Planet Search (MPS) collaboration. The MPS data constrain the first caustic crossing to have occurred after 1998 June 5.55 UT and thus directly rule out one of the two fits presented by the PLANET collaboration (model II). This substantially reduces the uncertainty in the the relative proper motion estimations of the lens object.

We perform joint binary microlensing fits of the MPS data together with the publicly available data from the EROS, MACHO/GMAN and OGLE collaborations. We also study the binary lens fit parameters previously published by the PLANET and MACHO/GMAN collaborations by using them as initial values for χ^2 minimization. Fits based on the PLANET model I appear to be in conflict with the GMAN-CTIO data. From our best fit, we find that the lens system has a proper motion of $\mu = 1.3 \pm 0.2 \text{ km s}^{-1} \text{ kpc}^{-1}$ with respect to the source, which implies that the lens system is most likely to be located in the Small Magellanic Cloud strengthening the conclusion of previous reports.

Subject headings: dark matter - gravitational lensing - Stars: low-mass, brown dwarfs

¹Department of Physics, University of Notre Dame, Notre Dame, IN 46556

²Departments of Astronomy and Physics, University of Washington, Seattle, WA 98195

³Center for Particle Astrophysics, University of California, Berkeley, CA 94720

⁴Mt. Stromlo and Siding Spring Observatories, Australian National University, Weston, ACT 2611, Australia

⁵Tate Laboratory of Physics, University of Minnesota, Minneapolis, MN 55455

1. Introduction

The Microlensing Planet Search (MPS) Project monitors microlensing events discovered in progress by the EROS, MACHO, and OGLE experiments in search for the microlensing signature of planets orbiting faint lens stars or “non-standard” microlensing light curves which can provide an additional constraint on the distance and mass of the “dark” lens systems. The MPS project primarily monitors lensing events toward the central regions of the Galaxy where the microlensing events are most numerous. However, “non-standard” events detected towards the Magellanic Clouds present a unique opportunity to learn about the composition of the dark halo that dominates the mass of the Milky Way, and these events are observed at a high priority. The binary microlensing event MACHO-98-SMC-1 was one such case.

The measurements of the microlensing optical depth towards the Large Magellanic Cloud (LMC) indicates that there is a previously unknown “dark lens population” toward the LMC (Alcock et al. 1997a). If the microlensing population is dominated by Galactic halo objects, the time scale of the microlensing events indicates their typical mass to be $\sim 0.5M_{\odot}$, which may be low mass stars, white dwarfs, or primordial black holes (Nakamura et al. 1998). A large population of low mass stars or white dwarfs in the Galactic halo would likely have other observable effects, and it has been speculated that the LMC microlensing events are due to normal stars in the LMC itself (Sahu 1995). The possible confusion between LMC self-lensing and lensing by Galactic halo objects derives from the fact that the distance and the mass of the lensing objects cannot be directly measured for most of the microlensing events. For a “standard” microlensing event, the only constraint on the three unknowns of distance, velocity and mass of the lens system comes from a single observed quantity, the “Einstein ring radius crossing time” t_E .

In a caustic crossing binary lensing event, one can measure one more independent parameter, namely, the “source radius crossing time”, t_* , and thereby estimate the relative proper motion μ of the lensing object with respect to the source star by independently determining the angular size of the source star from its brightness and color. A measurement of the relative proper motion, μ , allows the determination of the angular Einstein ring radius, $\theta_E = \mu t_E$. Once θ_E is known, the mass of the lensing object is expressed as a simple monotonic function of the distance to the lens (if the distance to the source is known). If D_{ℓ} and D_s are the distances to the lens and the source star, and $\delta \equiv D_{\ell}/D_s$, then

$$\left(\frac{M}{M_{\odot}}\right) = \frac{\delta}{1-\delta} \left(\frac{D_s}{60 \text{ kpc}}\right) \left(\frac{\theta_E}{0.369 \text{ mas}}\right)^2. \quad (1)$$

D_{ℓ} is not known, but it is strongly correlated with the proper motion, μ . For example, if we take our best fit value of $t_E = 70.5$ days and assume $D_s = 60$ kpc and $\mu = 1 \text{ km s}^{-1} \text{ kpc}^{-1}$, then the lensing object will be a binary in the SMC with the total mass $M \approx 0.36M_{\odot}$ for $D_s - D_{\ell} = 2$ kpc. For a typical halo lens we expect $D_{\ell} \approx 10$ kpc and a transverse velocity of $\approx 200 \text{ km s}^{-1}$ assuming a standard isothermal sphere halo model (Binney & Tremaine 1987). This yields $\mu \approx 20 \text{ km s}^{-1} \text{ kpc}^{-1}$ for a typical halo lens (which would imply a lens mass of $M = 0.81M_{\odot}$ from eq. 1.) Of course, in

order to compare to our measurement of μ , we should compare to the predicted μ distributions for halo and SMC lenses. This has been done for some simple SMC and halo models by Graff & Gardiner 1998; Albrow et al. 1998; Alcock et al. 1998; Honma 1998, and their results indicate that for most values of μ , either a halo or SMC lens is strongly preferred. However, depending on the halo and SMC models used, there is an overlap region at $\mu = 2 - 4 \text{ km s}^{-1} \text{ kpc}^{-1}$ which is marginally consistent with either a halo or SMC lens at the $2 - 3\sigma$ confidence level. (Honma (1998) also points out a selection effect that will tend to bias μ measurements towards smaller values.) In the case of MACHO-98-SMC-1, model II of the PLANET collaboration (Albrow et al. 1998) yields $\mu = 2 \text{ km s}^{-1} \text{ kpc}^{-1}$ which does not allow a definite determination of the lens location in the halo or in the SMC (Honma 1998).

The main features of a binary lensing event are determined by the location of the caustic curve in the source plane indicates the location of the source with respect to the lens system projected to the position of the source. The caustic curve is where the number of images of the source changes by two. In binary lensing, the caustic curve is made of one, two, or three closed curves, and the number of images is 5 inside the closed curves and 3 outside. The caustic curves for MACHO-98-SMC-1 (according to the MPS fit) are shown in Figure 1. When the source moves inside one of these caustic curves, two new images are created, and the magnification of these new images is singular at the point of the caustic crossing. Because of this discontinuity (intrinsic width zero), the finite angular size of the source star is *necessarily* resolved during a caustic crossing. At the same time, this discontinuity makes it difficult to observe the first caustic crossing (going into the caustic). However, there is always the second opportunity to monitor a caustic crossing once the first caustic crossing has occurred because of the closedness of the caustic curve, and the second caustic crossing (exit from the caustic) time can be predicted through real-time data reduction and binary lens fitting as the source proceeds inside the caustic. The timely pre-caustic crossing announcements from the MACHO/GMAN group (Becker et al. 1998; Bennett et al. 1998a) allowed intense monitoring of the second caustic crossing of the MACHO-98-SMC-1 by the microlensing community around-the-clock from all three (temperate) continents of the Southern Hemisphere (Afonso et al. 1998; Albrow et al. 1998; Alcock et al. 1998). This resulted in a light curve which is well sampled in the second caustic crossing region.

According to our fit, the binary lensing event MACHO-98-SMC-1 was magnified by ≈ 70 times at the maximum of the second caustic crossing. Such extreme magnification is also useful in studying the properties of the lensed star (Lennon et al. 1996; Alcock et al. 1997c). In order to obtain an accurate model of the lensing event, which is necessary to determine μ , however, it is not enough to have only meticulous measurements of the second caustic crossing. The main contribution of the MPS data is to constrain the time of the poorly sampled first caustic crossing and directly rule out the “outlier” PLANET model II.

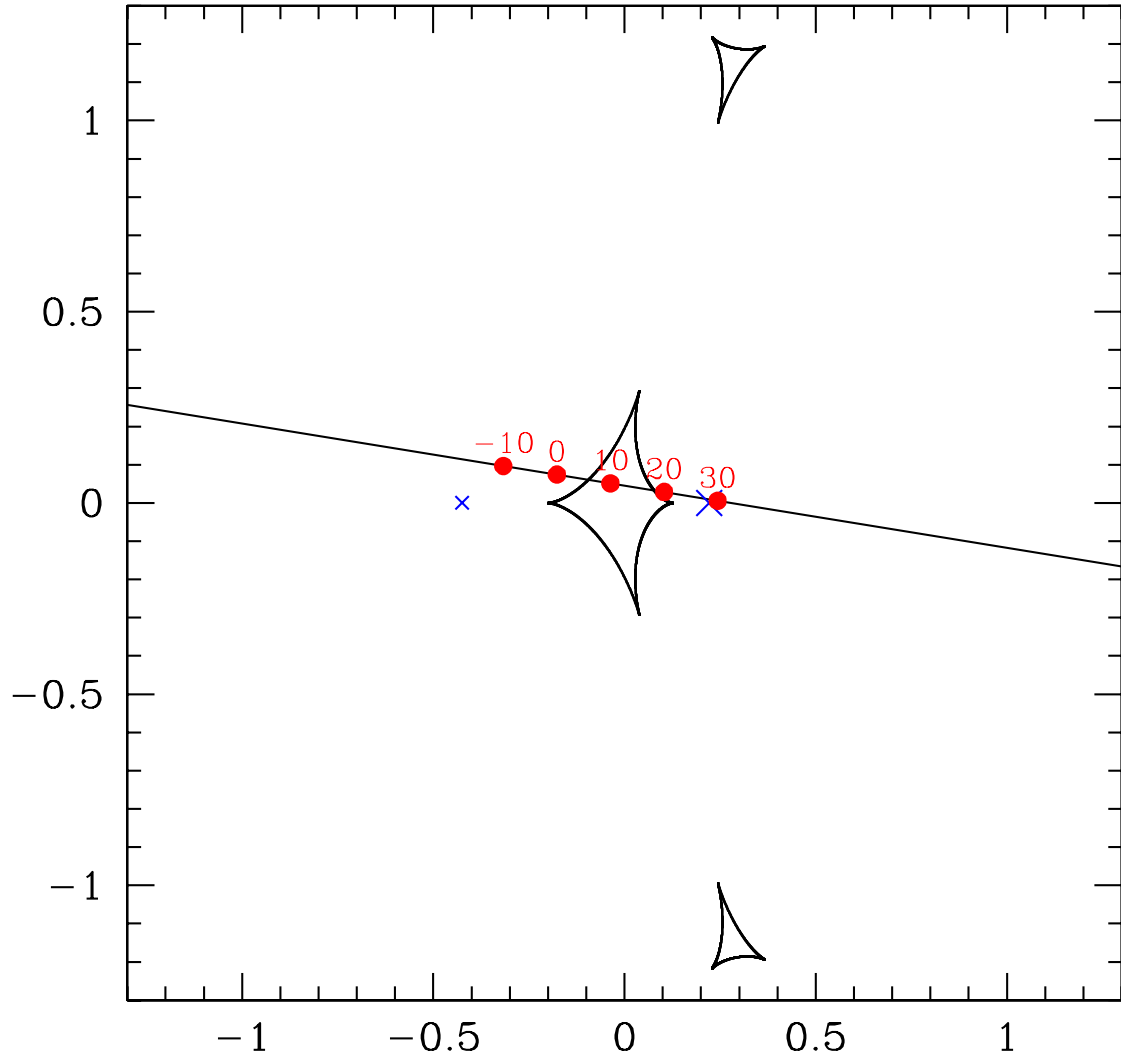


Fig. 1.— This figure shows the configuration of the caustic curves for the MPS lightcurve fit to binary lensing event MACHO-98-SMC-1. The crosses indicate the locations of the lenses, and the straight line indicates the path of the source star with respect to the caustic curves. The red dots on the source star path indicate the location of the source at various dates given in June, UT. The distance scale for the axes is the Einstein ring radius, R_E . Note that the actual size of the source star is only about $0.0015R_E$ that is much less than the thickness of the curves in the Figure.

2. MPS Observations and a Constraint on the First Caustic Crossing

The Microlensing Planet Search project has been allocated approximately 100 nights on the Mt. Stromlo Observatory (MSO) 1.9m telescope for the 1997 and 1998 Galactic bulge seasons. Ongoing microlensing events announced by the MACHO, OGLE, and EROS collaborations are monitored at intervals of 1-2 hours using the Monash Camera which is a Cassegrain imager fitted with a SITe 15 micron 2048 x 4096 AR-coated thinned CCD. The data is reduced within a few minutes after it is taken using automated Perl scripts written by one of us (ACB) which call a version of the SoDOPHOT photometry routine (Bennett et al. 1999). This allows the immediate discovery of any unusual microlensing features that might be in progress.

MPS made its first observation of event MACHO-98-SMC-1 about one day after MACHO microlensing alert issued May 25.9 UT and continued its observations as a medium priority target. One of these observations was obtained at June 5.549 UT which turned out to be the last observation prior to the caustic crossing. After the caustic-crossing binary lensing alert issued June 8.99 UT, MACHO-98-SMC-1 was upgraded to a high priority target. However, we were not scheduled on the MSO 1.9m until June 18, so our coverage of the event while the source was inside the caustic curve was minimal. On the 18th, the imager was available again, and the MSO staff kindly altered the telescope pointing limits to allow us to observe the SMC almost completely under the pole at an airmass of 3.2. We made the first observation at June 18.332 UT about 40 minutes after the trailing limb of the star cleared the caustic (according to our best fit which indicates the second caustic crossing endpoint at June 18.304 UT). Although we missed the second caustic crossing, we kept MACHO-98-SMC-1 at a high priority to cover the “cusp approach” lightcurve feature. This was a rise to a gentle peak and subsequent decline that occur as the source passes in front of one of the sharp “cusps” of the caustic curve (see Figure 1). Good coverage of this feature is important if we hope to constrain the global parameters of the lensing event. Unfortunately, due to poor (la Niña) weather, our coverage of the “cusp approach” is not very good.

The intense worldwide monitoring of the event was concentrated around the second caustic crossing making it the best covered caustic crossing in microlensing history. However, a reasonable amount of data around the first caustic crossing is necessary to pin down the lens parameters. The OGLE observation June 6.40 UT and the MACHO/GMAN observation at June 6.45 UT that indicate that the first caustic crossing must have occurred by June 6.0 or so. A lower limit on the time of the first caustic crossing is set by the MPS observation at June 5.549 UT which is the last observation before the first caustic crossing. The measured flux of this MPS observation is consistent with the slow variation of the lightcurve for a source approaching a binary caustic prior to the first contact of the caustic with the stellar limb. Thus, the first caustic crossing is constrained to have been completed within the window of ~ 20 hours between June 5.55 - 6.40 UT.

3. Binary Lensing Analysis

A binary lensing event involves seven parameters. These include three parameters that also exist for single lens events: the Einstein ring crossing time, t_E , the “impact distance,” u_{\min} , from the origin of the coordinate system, and the time of the closest approach to the origin, t_0 . We choose the lens system center of mass (c.m.) as the origin so that t_0 would be the most reasonable generalization of the time for the maximum amplification of a single lens. (The c.m. resides inside the caustic here. It always does when $a \leq \sqrt{2}$.) This would also be the most convenient coordinate system if we were to consider the lens system orbital motion. There are three additional parameters intrinsic to a binary lens: the fractional mass, ϵ , of the first lens, the lens separation a , and the intersection angle of the source trajectory with the lens axis, θ . (The first lens is the one on the left in Figure 1). The final parameter is the source radius crossing time t_* which is obviously critical for the lens proper motion determination.

In addition to these microlensing parameters, we must have additional parameters to describe the unlensed brightness of source star in each pass band, from each observing site (since the instrumental pass bands from different telescopes are never identical). Also, since the microlensing events are found in crowded stellar fields, it is usually the case that the lensed source is blended with other unlensed sources that happen to fall within the same seeing disk. Thus, we require an additional parameter for the brightness of any unlensed sources which are blended with the lensed source. These parameters need not be included for the non-linear χ^2 minimization process, however, because the observed flux depends linearly on the brightness of lensed star and its unresolved companions. Our χ^2 calculation routine automatically minimizes χ^2 with respect to these linear parameters for every set of intrinsic microlensing parameters that is considered. This makes our fitting routine converge to the best fit much more quickly than it would if these were included as nonlinear fit parameters. However, it also complicates the interpretation of our error estimates because the error estimates for the blending parameters are calculated with the intrinsic lensing parameters held fixed.

When a source is inside a caustic curve, there are two extra images in addition to the three “normal” images, and when the caustic curve crosses the source star, the two extra images are only partial images joined together along the critical curve. The time it takes for the stellar diameter to cross the caustic, $2\Delta t$, can be measured using only observations near the time of the caustic crossing. However, t_* can be determined from Δt only if we know the angle, ϕ , between the source trajectory and the caustic curve at the crossing: $t_* = \Delta t \sin \phi$. ϕ can only be determined by a fit to the entire microlensing lightcurve, so measurements of the caustic crossing alone are not sufficient to determine t_* . It is possible to constrain t_* without a determination of ϕ (Afonso et al. 1998), but this constraint may be very weak.

The modeling of a binary lensing event presents a number of difficulties. First, the caustic crossings mean that binary lensing lightcurves generically have very sharp features, and since the photometric measurements discretely sample the lightcurves, there can be large changes in

χ^2 caused by small changes in the parameters that happen to move a caustic past the location of a data point. The singular nature of microlensing magnification also causes difficulties for the integrations necessary to calculate the microlensing magnification of a finite size source star and prevents the use of fast high order methods (Rhie & Bennett 1999).

Yet another difficulty with binary lens fits is that the location of the caustic crossing in the lightcurve depends in a complicated way on the microlensing parameters. The time of the caustic crossings can generally be pinned down to reasonable accuracy simply by inspection of the microlensing lightcurves, but it is difficult to translate this into a constraint on the microlensing parameters: ϵ , a , θ , u_{\min} , t_0 , and t_E . However, since the times of the caustic crossings can readily be calculated for any set of parameters, it is possible to shift t_0 and rescale t_E to put two caustic crossings at specified locations in time. We use such a procedure to replace the parameters t_0 and t_E by the first and second caustic crossing times, t_{cc1} and t_{cc2} , for many of our binary lens fits.

The χ^2 minimization for our microlensing fits is carried out with the aid of the MINUIT routine (James 1994). The fitting proceeds in several stages. First, in order to find candidate global fits, we take the data sets and remove many of the data points from regions where the data highly oversample the lightcurve features in order to speed up the calculations in the early phases of the fitting process. We also remove all of the data points which resolve the caustic crossing so that the search for candidate global microlensing fit parameters can be done in the point source limit which typically speeds up the calculations by a factor of 10 or more. We then start a number of Monte Carlo parameter searches to find good starting points for the microlensing fits using MINUIT's SEEK routine. During the Monte Carlo parameter searches, the values of t_{cc1} and t_{cc2} are constrained to small time intervals which were determined by inspection of the individual lightcurves. This results in a number of candidate microlensing models which are passed to the second stage of the fitting procedure.

In the second stage of the fitting process, we include some of the data which resolves the caustic crossing and to fit all of the candidate microlensing models again with a finite value for t_* . This procedure converges to the final fit much more quickly than if all the data were used at this stage. Once the finite source effects are included, it is necessary to take the limb darkening of the source into account. For our preliminary fits, we have used a standard “linear” limb darkening model, but we have also used the “square-root” model advocated by Diaz-Cordoves & Gimenez (1992) at the stage of the final fits which use the full data set. The limb darkening coefficients were taken from Claret, Diaz-Cordoves, & Gimenez (1995) and Diaz-Cordoves, Claret, & Gimenez (1995).

In addition to this procedure used to find new fits, we have also tried fits using initial conditions based upon the fits reported by the PLANET and MACHO/GMAN collaborations.

3.1. Previous Observations, Analyses, and Fits

Observations of MACHO-98-SMC-1 have been previously presented by the EROS, PLANET, MACHO/GMAN, and OGLE collaborations. (Afonso et al. 1998; Albrow et al. 1998; Alcock et al. 1998; Udalski et al. 1998) The EROS observations from La Silla covered a significant fraction of the falling curve of the second caustic crossing through the caustic crossing “end point” and several hours beyond, and it was the first time that the linearity towards the “end point” was observed. At the “end point”, the source star completely exits the caustic, and the additional two bright partial images vanish, causing the curvature of the light curve to change abruptly. The “end point” was estimated to have occurred June 18.297 UT. From the linearity spanning 1.8 hours, the EROS collaboration suggested a constraint $\mu \sin \phi \lesssim 1.5 \text{ km s}^{-1} \text{ kpc}^{-1}$. Since they reported on data only from the night of the second caustic crossing, EROS was not able to determine the caustic crossing angle ϕ , so their constraint on the lens proper motion was weak. However, the EROS data has the best coverage of the caustic crossing “end point” which proves very valuable when combined with other data sets.

The PLANET collaboration monitored the event since shortly after the binary lens alert and had excellent coverage of the second caustic crossing peak turn-over from the SAAO 1m. They also measured the spectrum at the light curve peak from the SAAO 1.9m. They presented two binary lens fits, which we will refer to as PLANET-I and PLANET-II, that resulted in $t_* = 0.122$ and 0.0896 days. The models PLANET-I and II differ by ~ 58 in χ^2 which is formally a 7.6σ deviation. However, the χ^2 per degree of freedom for each were fairly large (2.37 and 2.73 respectively), and they argued that both the fits should be considered to be viable fits (to account for unspecified systematic errors).

The MACHO/GMAN group reported their data from the Mt. Stromlo 1.3m and the CTIO 0.9m telescopes (Alcock et al. 1998) and presented a binary microlens fit to the data combined with the EROS data. Their fit differed from both PLANET-I and PLANET-II, and MACHO/GMAN suggested that both the PLANET models might be inconsistent with pre-caustic-crossing MACHO/GMAN data. Their estimate of the source radius crossing time was $t_* = 0.116$ days. The CTIO 0.9m observations registered the caustic crossing “end point” at \approx June 18.304 UT which agrees with the EROS data reduced with SoDOPHOT (see figure 4). The MACHO/GMAN fit indicates that the second caustic crossing peak amplification was ≈ 70 while PLANET-I indicates that the maximum amplification was ≈ 100 . The main difference here is that the the PLANET-I indicates a fainter source star with more of the baseline flux coming from unlensed stars.

The OGLE collaboration reported their data from Las Campanas (1.3m Warsaw telescope) that includes the first observation after the first caustic crossing at June 6.40 UT. They did not perform any microlensing fits, but they suggested that model PLANET-I is more consistent with the OGLE data than PLANET-II. They also suggested that MACHO/GMAN fit may be off by 0.14 days for the first caustic crossing. In the MACHO/GMAN fit, the first caustic peak crossing occurred at \approx June 6.24 UT, and hence, the suggestion by the OGLE team corresponds to the

first caustic peak crossing at \approx June 6.10 UT. In model PLANET-I, the peak crossing time was \approx June 6.08 UT, and thus, the OGLE team concluded that the OGLE data is probably most consistent with model PLANET-I.

3.2. MPS fits, Analyses, and Comparison

In this section we present our binary microlensing fit results for the data set including the MPS data plus the publicly available MACHO/GMAN, EROS, and OGLE data, and we interpret the meaning of these results. We assume that the source star is a single lens star which was lensed by a binary lens with no significant orbital motion.

The most obvious result of the MPS observations is that the PLANET-II model is ruled out. The MPS observation at June 5.55 UT indicates that the leading limb of the source star has not yet crossed the caustic. This is inconsistent with the PLANET-II model which predicts the leading limb to cross the caustic at June 5.25 UT, the stellar center “caustic crossing time” at June 5.36 UT, and the first caustic crossing lightcurve peak to occur at June 5.43 UT. Figure 2 shows a comparison of the PLANET-II fit to the MPS data. In order to put it into the statistical perspective, we normalize the MPS data to the PLANET-II fit using the 34 other observations (which do give an acceptable fit to the data), and the PLANET-II prediction for June 5.55 UT exceeds the observed brightness by 29σ . Thus, the PLANET-II model is clearly ruled out. Note that in Figure 2 and in all subsequent plots, the MPS data have been binned into nightly bins for all nights with multiple observations except for the night of June 18 where 16 observations have been grouped into 4 bins.

The MPS observation on June 5.55 along with the OGLE observation at June 6.40 UT and the GMAN-CTIO observation at June 6.45 constrain the caustic crossing to have occurred close to June 6.0 UT. The MPS fit to the combined data set provides an acceptable fit to the data near the first caustic crossing and indicates that the first “caustic crossing time” was June 5.91 UT, and PLANET-I and MACHO/GMAN also seem consistent with this data within the limit of the poor coverage. Therefore, we will focus on a comparison between the MPS, MACHO/GMAN and PLANET-I fits as well as the lightcurve details of the second caustic crossing where we hope to reconstruct the “missing peak.” (A future comparison with the PLANET data should test our ability to predict the features of the second caustic crossing peak from the other data sets which do not sample the peak.)

Tables 1-4 shows the summary of the results of the microlensing fits we have performed on the combined EROS/GMAN/MACHO/MPS/OGLE data set. The MPS fit is the fit generated by our fit search procedure as discussed above. The fits labeled “PLANET-I*” and “MACHO/GMAN*” are fits in which we started with the binary lens parameters reported by these groups as initial conditions. The columns labeled “PLANET-I” and “PLANET-II” report results for the fit parameters found by the PLANET collaboration; the only additional fitting was to find the best

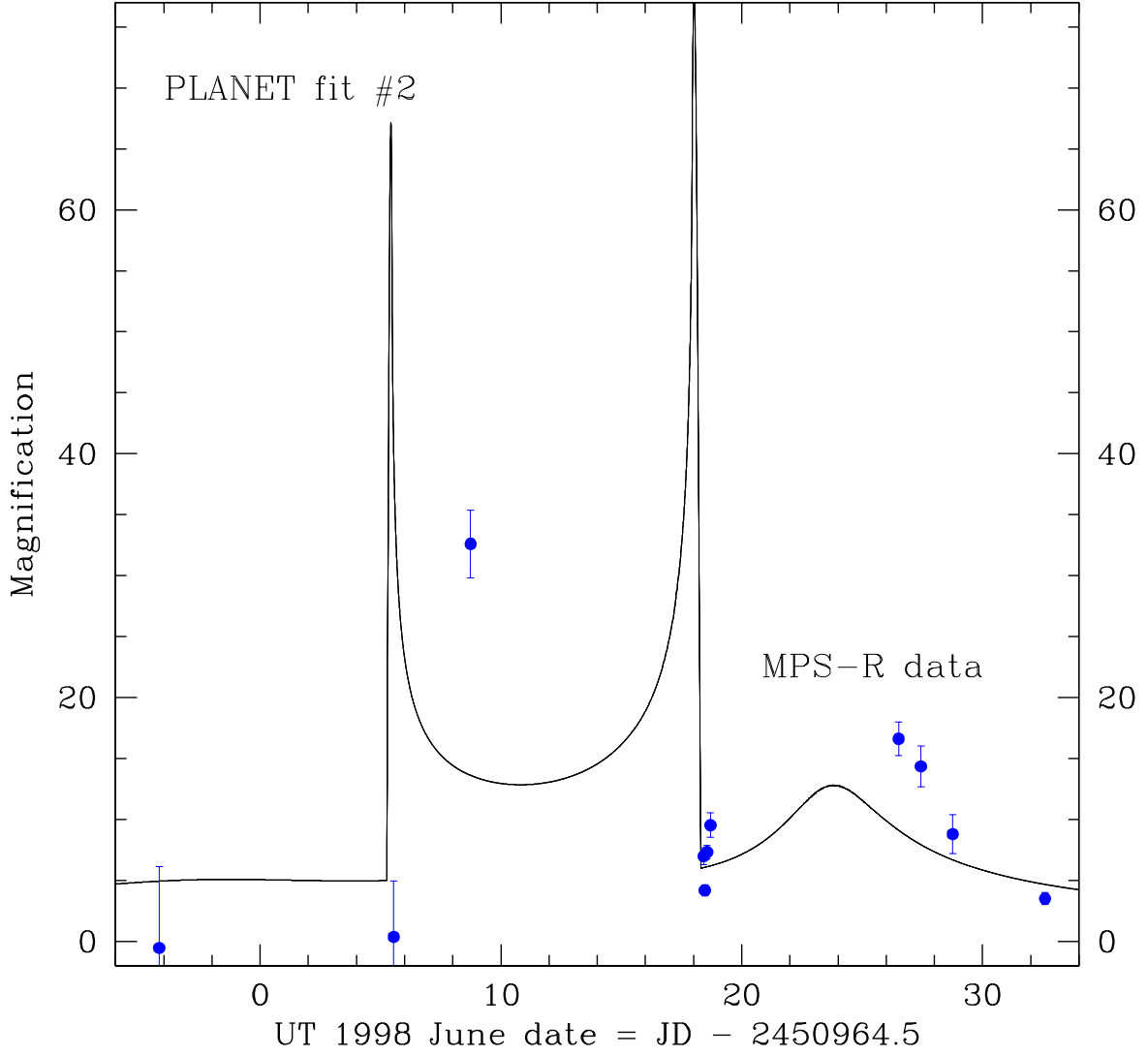


Fig. 2.— This figure shows a comparison of the MPS data to the PLANET-II fit. We have allowed the fluxes of the source star and any unlensed stars in the same seeing disk to take the values which give the lowest χ^2 value. The observation at June 5.55 UT indicates that the caustic crossing had not yet begun, contrary to the PLANET-II model prediction. The attempt to fit this point results in a “best-fit” curve which does not agree with most of the other data points.

fit fluxes for the lensed star and its unresolved companions.

The blend fractions or “fractional lensed luminosity” values listed in Table 3 require some explanation. These blend fractions have large uncertainties for many of the passbands because there are few or no observations when the source is not magnified significantly for most of the pass bands. The only tight constraint on the unlensed flux comes from the MACHO data where there are more than 600 observations in both MACHO pass bands when the source is unmagnified. The f_s values in Table 3 can also depend on the seeing of the best images from each of the data sets. With routines such as DOPHOT, SoDOPHOT or ALLFRAME, the photometry is based upon the stars that can be individually identified in the best seeing frames. Thus, two data sets using the nearly identical passbands can yield different f_s values if the seeing in the best seeing frames differs between the two data sets.

Table 1 shows the summary of the lens parameters and statistics. t_{cc1} and t_{cc2} refer to the first and second caustic crossing times which are fit parameters for the MPS fits but not for the MACHO/GMAN or PLANET-I fits. The caustic crossing times appear to agree well between the different fits. The MACHO/GMAN and MPS fit parameters agree in general except in the mass ratio, but these fits differ more substantially from the PLANET-I fit. Of course, this is not very surprising since the MACHO/GMAN and MPS fits are based on data sets that have a lot of overlap with each other but no overlap with the data that generated the original PLANET-I fit.

Much of the difference between the PLANET-I and MACHO/GMAN and MPS fits can be traced to the fact that the PLANET-I fit indicates more blending. In other words, the lensed source implied by the PLANET-I model is fainter and has brighter unlensed neighbors than in the MACHO/GMAN and MPS models. This can be seen from the best fit blend fractions listed in Table 3. The fraction of the lensed light is $f_s(V_m) \simeq 0.57$ and $f_s(R_m) \simeq 0.49$ for the MACHO/GMAN and MPS fits of the MACHO data while for the PLANET-I fit the values are $f_s(V_m) \simeq 0.35$ and $f_s(R_m) \simeq 0.30$. So, the MACHO/GMAN and MPS fits imply that the lensed source is about half a magnitude brighter than implied by the PLANET-I fit. It is interesting to note that the χ^2 difference between the MACHO/GMAN and MPS fits and the PLANET-I fit is seen only in the MACHO and CTIO data sets, which are also the data sets in which the unmagnified fit fluxes are the same for the different fits. For the EROS, MPS, and OGLE data, the unmagnified brightness of the blended stellar image is predicted to be substantially fainter for the PLANET-I fit than for the MACHO/GMAN and MPS fits. Thus, additional data from EROS, MPS, OGLE, and perhaps PLANET as well should help to distinguish between these fits.

The form of the fit curves near the caustic crossings depend on the assumed form for the limb darkening. Following the PLANET collaboration, the PLANET-I and PLANET-II χ^2 results reported here assume no limb darkening. For most of the fits that we’ve done, we have assumed the common “linear” limb darkening model, but the fit labeled MPS-sqrt was done using the square-root model of Diaz-Cordoves & Gimenez (1992) which is expected to be more accurate. The parameters used for each pass band are listed in Table 4, and they are appropriate for a star

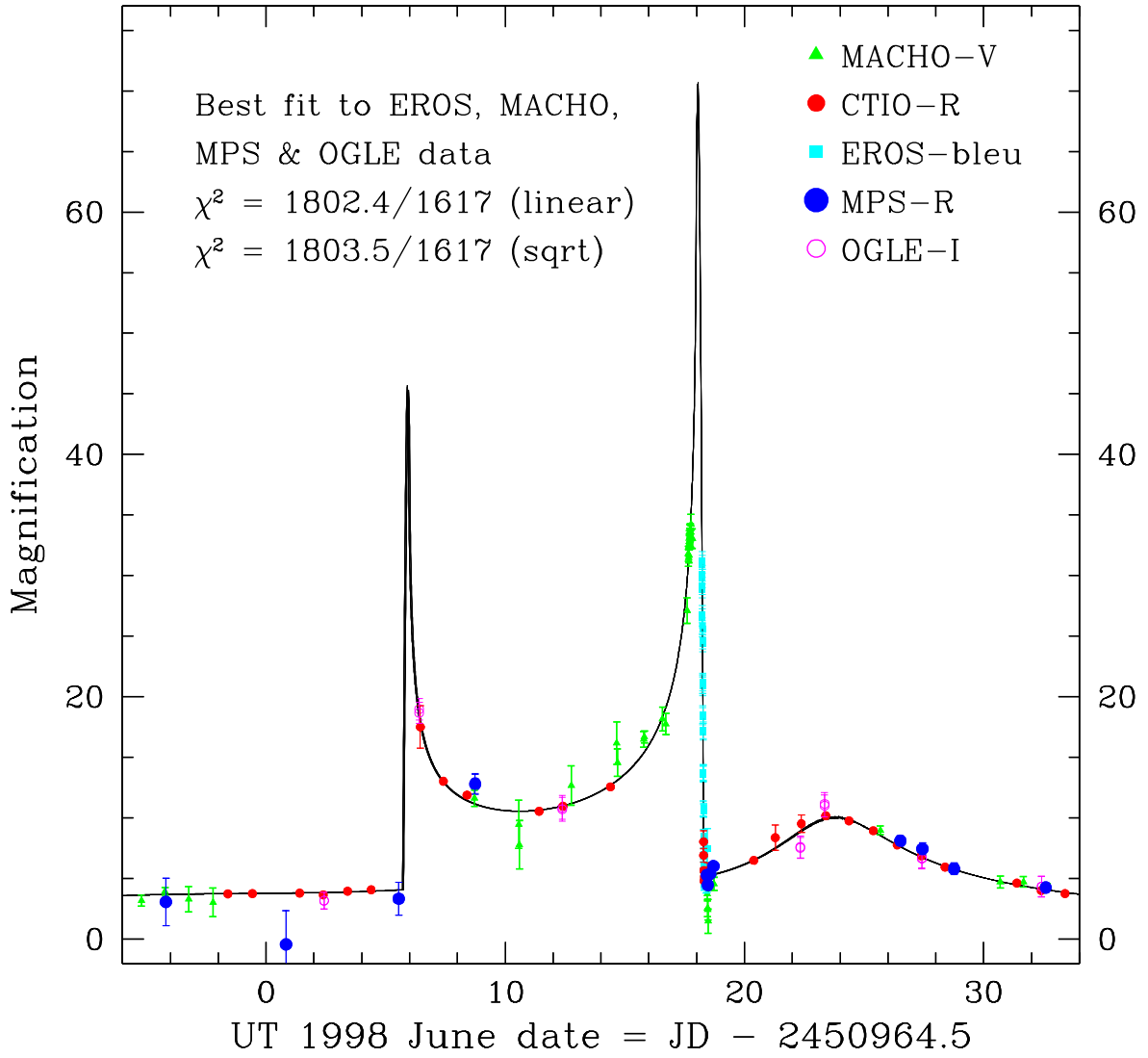


Fig. 3.— This figure shows the MPS fit using the square root and linear limb darkening models. The EROS-rouge, MACHO-V, and CTIO-B data are not shown. The MPS fits with linear and square root limb darkening models are indistinguishable on this plot.

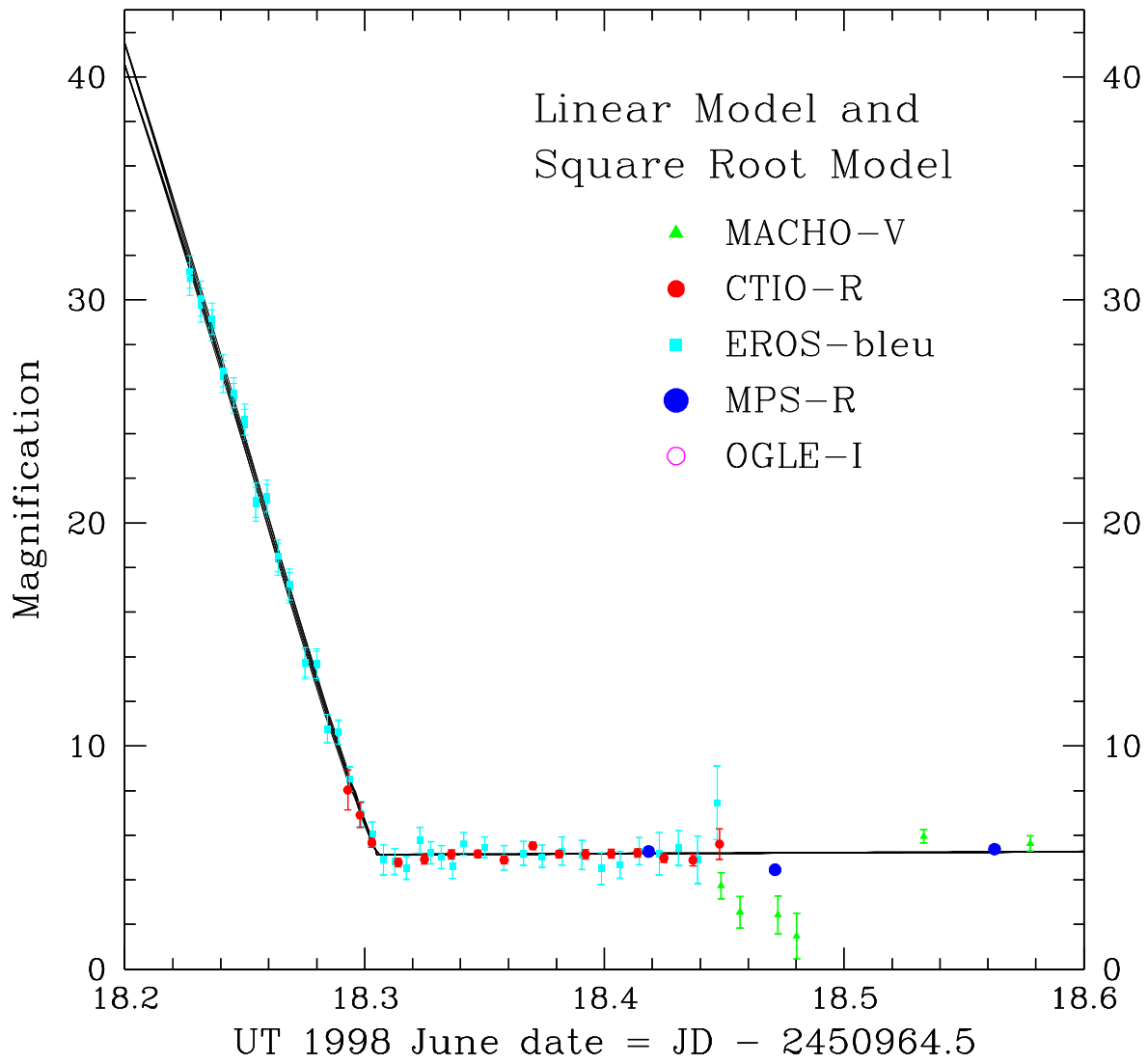


Fig. 4.— This figure shows the 2nd caustic crossing endpoint MPS fit using the square root and linear limb darkening models. The square root model is the one that predicts a slightly lower magnification at June 18.20.

with an effective temperature of $T = 8000K$ and a surface gravity of $\log g = 4.5$. (See section 3.3 for a discussion of the properties of the source star.)

The modeling of the lightcurve near the second caustic crossing peak is subject to some systematic uncertainty due to the features and limitations of the MACHO and EROS data which bracket the peak. The MACHO/GMAN paper noted that there is an apparent lightcurve deviation near June 17.7 that might be explained as a caustic crossing due to a faint companion to the source star. Another possible explanation might be systematic photometric errors. In either case, this deviation will add to the uncertainty in our prediction for the lightcurve during the missing peak of the caustic crossing. Another contribution to this uncertainty is the fact that the publicly available EROS data was all taken on the night of the caustic crossing. It includes the last half of the caustic crossing, but there are no other lightcurve features visible in this data set. Thus, the modeling of the EROS data will be quite sensitive to possible errors in the limb darkening model. Because of these potential problems, we include an additional systematic error of ± 0.1 for our measurement of t_* .

The timing of the second caustic crossing is seen to be very close to the last pre-caustic crossing prediction from MACHO/GMAN: $t_{cc2} = \text{June 18.18 UT}$ vs. the prediction of June 18.2 UT (issued via email on June 17).

The peak magnification of the caustic crossing is predicted to have occurred at June 18.055 for the MPS-linear fit and June 18.045 for the MPS-sqrt fit. The lightcurve peak assumed by PLANET seems to be earlier than this by ~ 0.03 days which agrees with our prediction when we account for the systematic errors mentioned above.

As a way to judge the overall merit of the different lightcurve fits, we compare the fit χ^2 values for each of the models. The MPS-linear and MPS-sqrt χ^2 values differ by only 1.5 which is not statistically significant. The χ^2 value for the MACHO/GMAN fit is larger than the MPS-linear value by 21.3 which is formally equivalent to a 4.6σ deviation while the χ^2 value for the PLANET-I fit is larger by 85.9 or 9.3σ . Thus, the PLANET-I fit is clearly disfavored, but it is premature to dismiss it as we have not yet included the PLANET data itself in our fits. The inclusion of the PLANET data plus additional data from the other groups in our fits should resolve this question, however.

3.3. Source Star Characterization

In order to estimate the proper motion from the microlensing fits, we must estimate the angular radius of the source star. This can be accomplished with estimates of the stellar temperature, brightness and the amount of extinction. The brightness estimate depends on the amount of blending as determined by the binary microlensing fit, but the temperature and extinction can be estimated from the broad band colors and a spectrum. The PLANET collaboration has spectrum from the SAAO 1.9m near peak magnification which indicates that the

source star is an A star with $T \approx 8,000$ K. The color of the star has been estimated by PLANET to be $V - I = 0.31 \pm 0.02$ while MACHO estimates $V - R = 0.03 \pm 0.03$. These colors are somewhat difficult to reconcile, and we suspect that one or both color estimates may be subject to systematic errors larger than the estimates above. If we attempt to find a reasonable fit to both color estimates, then we must assume a relatively small amount of extinction to be consistent with the MACHO color and the PLANET spectrum. We take $A_V = 0.12 \pm 0.1$.

From the MACHO photometric calibrations and the MPS fit, we estimate the unlensed magnitude of the source at $V = 21.98$, and if we use the PLANET photometric zero point, we get $V = 21.91$. We adopt $V = 21.95 \pm 0.15$. The source star is expected to be a member of the SMC, but if the lens is in the SMC as well, then the source star is likely to be located on the far side of the SMC. Since it does appear that the lens is likely to be located in the SMC, we will assume a distance of 62.5 ± 2.5 kpc to the source. This yields an absolute magnitude of $M_V = 2.85 \pm 0.2$. From the Bertelli et al. (1994) isocrones, we see that this is compatible with a metal poor ($[\text{Fe}/\text{H}] = -1 \pm 0.3$) A star with a radius of $\theta_* = 8.2 \pm 0.8 \times 10^{-8}$ arc sec, or $R = 1.1 \pm 0.1 R_\odot$ assuming a distance of 62.5 ± 2.5 kpc. Our best fit value for $t_* = 0.108$ days (using the square-root limb darkening model), but this value is sensitive to uncertainties in the blending for the EROS data. The publicly available EROS data consists of only data taken on the night of the caustic crossing, and it has essentially only two features: a linear decline followed by a period of constant brightness. This means that if we fit only the EROS data with an unknown amount of blending, there will be a fit degeneracy that will allow a change in the caustic crossing time scale to be compensated by a blending change. This will be constrained by the shape of the fit curve in other pass bands near the caustic crossing peak, but the MACHO data seems to show an anomaly near the peak. Because of these uncertainties, we will add an additional 0.015 days as a systematic uncertainty to our measurement of t_* . This yields $\mu = 1.31 \pm 0.22 \text{ km s}^{-1} \text{ kpc}^{-1}$ and $\hat{v} = 82 \pm 14 \text{ km s}^{-1}$. These are consistent with the μ and \hat{v} estimates from the PLANET-I and MACHO/GMAN models, but it is substantially less than proper motion predicted from the PLANET-II model (Albrow et al. 1998; Alcock et al. 1998).

4. Conclusions

The MPS data adds a constraint on the first caustic crossing and rules out PLANET-II model. Since the PLANET-II model was the only proposed model which indicated a relative proper motion significantly different from our value of $\mu = 1.31 \pm 0.22 \text{ km s}^{-1} \text{ kpc}^{-1}$, this result significantly decreases the uncertainty in μ . As discussed previously (Afonso et al. 1998; Albrow et al. 1998; Alcock et al. 1998) this proper motion value clearly favors a lens in the SMC, and it does not require that the SMC be tidally disrupted as seemed to be necessary for the PLANET-II model to make sense.

While our analysis clearly favors the MPS fit over the MACHO/GMAN and PLANET-I fits, it would be best to do joint fits with all of the available data before making a final judgment.

Particularly valuable would be the PLANET data and additional EROS data. One significant difference between the MPS and MACHO/GMAN fits and the PLANET-I fit is that the PLANET-I fit implies that the lensed source is more severely blended and is therefore significantly fainter. From Table 3, we see that PLANET-I fit predicts that only 35% of MACHO- V_m band flux is lensed while the MPS and MACHO/GMAN fits predict 58% and 56% respectively. Future HST images of the lensed star should resolve lensed star from its nearby unlensed companions and determine the correct blend fractions in the different pass bands.

While the observations of MACHO-98-SMC-1 have clearly established that the lens is in the SMC, the implications for the interpretation of the lensing excess seen by the MACHO Collaboration towards the LMC are not clear. The standard model of the LMC is that it is basically a disk galaxy that is inclined by about 27° from face on to the line of sight. Gould (Gould 1995) has showed that the microlensing optical depth of such a galaxy is constrained by its line of sight velocity dispersion. This suggests that the self-lensing optical depth of the LMC is quite small, but it is conceivable that the LMC disk is not the whole story. For example, Weinberg (1998) suggests that the tidal interactions of the LMC and the galactic disk might give the LMC a larger self-lensing optical depth, but it is not known if this suggestion is consistent with the observed line of sight velocity dispersion of the LMC $\approx 20 \text{ km s}^{-1}$ (Meatheringham et al. 1988).

Unlike the LMC, the SMC is thought to be extended along the line of sight, and some estimates of the self-lensing optical depth of the SMC (Afonso et al. 1998; Alcock et al. 1998) are very similar to the measured microlensing optical depth of the LMC. However, a recent n-body model of the SMC predicts a somewhat smaller microlensing optical depth (Graff & Gardiner 1998), although this prediction, $\tau_{SMC} = 0.4 \times 10^{-7}$, is larger than most predictions for τ_{LMC} . So far, there are two microlensing events detected toward the SMC: MACHO-98-SMC-1, discussed here, and MACHO-97-SMC-1 (Alcock et al. 1997b). It has been suggested that MACHO-97-SMC-1 might also be due to an SMC lens due to its long timescale (Palanque-Delabrouille et al. 1998). However, attempts to make this argument more quantitative have invoked the assumption that the lens is a main sequence star which can not be considered a consistent assumption in the context of the dark matter problem. There has also been one caustic crossing binary event seen towards the LMC (Bennett et al. 1996b), but the lightcurve sampling of this event was not sufficient to yield an unambiguous determination of the location of the lens system.

For MACHO-98-SMC-1, we have no such ambiguity because of the complete lightcurve coverage. We can conclude with high confidence that the lens system resides in the SMC. Since this is the only Magellanic Cloud event with a reliable location, we cannot reach any conclusion about the location of the other Magellanic Cloud events. Furthermore, the rate of binary lensing events discovered towards the Magellanic Clouds is only about 0.3 per year, so the current generation of microlensing surveys is not likely to solve this problem. Fortunately, there are plans for second generation microlensing surveys (Stubbs 1998) which should increasing the microlensing detection rate towards the Magellanic Clouds by more than an order of magnitude. This will generate a large enough sample of microlensing events *with* distance estimates to resolve the puzzle presented

by the microlensing results towards the LMC. MPS will contribute to this effort by expanding to include observations from the Boyden Observatory near Bloemfontein, South Africa in 1999.

Acknowledgments

It is our great pleasure to express our gratitude to the Mt. Stromlo Observatory for the observing time and the support of their staff. We especially thank Jan van Harmelen who arranged for the maximum telescope range beyond the horizon safety limits for extended observations of the MACHO-98-SMC-1 on the night of June 18th 1998. We thank the EROS, MACHO/GMAN and OGLE Collaborations for making their data available.

This research has been supported in part by the NASA Origins program (NAG5-4573), the National Science Foundation (AST96-19575), and by a Research Innovation Award from the Research Corporation. Work performed at MSSSO is supported by the Bilateral Science and Technology Program of the Australian Department of Industry, Technology and Regional Development. Work performed at the University of Washington is supported in part by the Office of Science and Technology Centers of NSF under cooperative agreement AST-8809616.

REFERENCES

Afonso, C., et al. 1998, A&A, 337, L17

Albrow, M. D., et al. 1998, ApJ, Submitted, astro-ph/9807086

Alcock, C., et al. 1997, ApJ, 486, 697

Alcock, C., et al. 1997, ApJ, 491, L11

Alcock, C., et al. 1997, ApJ, 491, 436

Alcock, C., et al. 1998, ApJ, Submitted, astro-ph/9807163

Becker, A. C., et al. 1998, IAU Circ., 6935, 1

Bennett, D., et al. 1996a, IAU Circ., 6361, 1

Bennett, D. P., et al. 1996b, in Nucl. Phys. B (Proc. Suppl.), Vol. 51B, 131 (astro-ph/9606012)

Bennett, D., et al. 1998a, IAU Circ., 6939, 1

Bennett, D., et al. 1999, in preparation

Bennett, D. P., & Rhie, S. H. 1996, ApJ, 472, 660

Bertelli, G., Bressan, A., Chiosi, C., Fagotto, F., & Nasi, E. 1994, *Astronomy and Astrophysics Supplement Series*, 106, 275

Binney, J., & Tremaine, S. 1987, *Galactic Dynamics*, Princeton University Press

Claret, A., Diaz-Cordoves, J., & Gimenez, A. 1995, *A&AS*, 114, 247

Claret, A., Diaz-Cordoves, J., & Gimenez, A. 1992, *A&A*, 259, 227

Diaz-Cordoves, J., Claret, A., & Gimenez, A. 1995, *A&AS*, 110, 329

Graff, D. S., & Gardiner, L. T. 1998, [astro-ph/9811394](#)

Gould, A., 1995, *ApJ*, 441, 77

Honma, M. 1998, [astro-ph/9811397](#)

James, F., 1994, CERN Program Library Long Writeup D506:
<http://wwwinfo.cern.ch/asdoc/WWW/minuit/minmain/minmain.html>

Lennon, D. et al. 1996, *ApJ*, 471, L23

Meatheringham, S. J. et al. 1988, *ApJ*, 327, 651

Nakamura, T. et al. 1997, *ApJ*, 487, L139

Palanque-Delabrouille, N., et al. 1998, *A&A*, 332, 1

Rhie, S. H., & Bennett, D. P. 1999, in preparation

Stubbs, A., 1998, [astro-ph/9810488](#)

Sahu, K. C., 1995, *Nature*, 370, 275

Udalski, A., et al. 1998, *Acta Astronomica*, Submitted, [astro-ph/9808077](#)

Weinberg, M. 1998, [astro-ph/9811204](#)

Table 1. Binary lensing parameters and Statistics

	PLANET I	PLANET I *	MACHO/GMAN *	MPS-linear	MPS-sqrt
t_{cc1}	~ 6.0	~ 6.0	~ 6.2	5.912	5.932
t_{cc2}	18.12	18.12	18.2	18.183	18.194
t_0 (Jun UT)	14.130	14.228 (96)	13.931 (15)	13.105	13.120
t_E (days)	108.4	108.91 (29)	73.76 (41)	70.52	70.47
a	0.58685	0.58288 (75)	0.66365 (84)	0.64635 (22)	0.6462 (20)
u_{\min}	0.03164	0.03185 (8)	0.04628 (12)	0.04434 (16)	0.04479 (19)
θ (rad)	-0.2060	-0.2019 (33)	-0.1803 (18)	-0.1603 (20)	-0.1611 (21)
ϵ	0.2221	0.2214 (42)	0.2793 (57)	0.3411 (27)	0.3423 (23)
t_* (days)	0.1216	0.1290 (8)	0.1156 (10)	0.1050 (13)	0.1076 (21)
χ^2 / (d.o.f)	1979.2/1617	1887.9/1617	1823.3/1617	1802.0/1617	1803.5/1617

Table 2. Fit χ^2 values for individual pass bands

	PLANET II	PLANET I	PLANET I *	MACHO *	MPS-linear	MPS-sqrt
MACHO R_m	926.2/704	944.0/704	938.4/704	921.5/704	917.6/704	918.8/704
MACHO V_m	783.0/712	795.6/712	786.2/712	763.8/712	762.8/712	763.9/712
CTIO R	88.0/84	103.8/84	59.6/84	44.4/84	30.2/84	30.7/84
CTIO B	31.9/22	31.5/22	18.0/22	10.4/22	9.3/22	9.2/22
EROS R	20.5/38	47.0/38	20.9/38	19.5/38	19.8/38	20.5/38
EROS B	14.9/38	34.7/38	11.5/38	12.2/38	11.5/38	10.8/38
MPS R	129.3/35	47.0/35	45.8/35	46.9/35	48.4/35	47.4/35
OGLE I	5.4/7	2.2/7	7.5/7	4.6/7	2.3/7	2.1/7

Table 3. Fractional Lensed Luminosity f_s

passband	PLANET II	PLANET I	PLANET I *	MACHO *	MPS-linear	MPS-sqrt
MACHO R_m	0.409 (5)	0.301 (4)	0.300 (4)	0.475 (6)	0.494 (6)	0.494 (6)
MACHO V_m	0.480 (5)	0.353 (4)	0.352 (4)	0.557 (6)	0.578 (6)	0.579 (6)
CTIO R	0.85 (7)	0.58 (4)	0.55 (4)	0.79 (5)	0.89 (6)	0.87 (6)
CTIO B	0.90 (17)	0.67 (12)	0.70 (13)	1.07 (20)	1.01 (18)	1.01 (18)
EROS R	1.17 (76)	1.07 (82)	1.35 (1.30)	0.83 (36)	0.82 (34)	0.89 (40)
EROS B	0.54 (7)	0.70 (15)	0.63 (12)	0.40 (4)	0.40 (4)	0.42 (4)
MPS R	0.07 (1)	0.42 (12)	0.42 (12)	0.57 (16)	0.55 (14)	0.55 (14)
OGLE I	1.5 (2.7)	1.2 (2.3)	0.14 (4)	0.39 (17)	1.17 (1.37)	1.11 (1.22)

Table 4. Limb Darkening Parameter ξ

passband	linear	square root-c	square root-d
MACHO R_m	0.467	0.071	0.562
MACHO V_m	0.600	0.119	0.682
CTIO R	0.491	0.081	0.582
CTIO B	0.662	0.116	0.775
EROS R	0.446	0.071	0.562
EROS B	0.545	0.1055	0.624
MPS R	0.491	0.081	0.582
OGLE I	0.401	0.043	0.510